Complex Forms Trajectory Tracking in Robotized Welding

Hadjira Belaidi[1], Abdarrahmane Belaidi[2]
[1]Electrical and Electronic institute
Signals and Systems Laboratory
Boumerdes, Algeria
[2]Hydrocarbon and chemical department
Robotics laboratory
Boumerdes, Algeria
{Hadjira983, abd_belaidi}@yahoo.fr

ABSTRACT: *Actually, in the majority of mechanical systems such as industrial robots, mobile robots with embarked structure, etc… the end-effector mass widely exceeds that of the supported load, and lot of works do not take it into account in their algorithms. These systems must be designed based on dynamic model; moreover the synthesis of the algorithm of an autonomous manipulator must be accomplished by taking into account nonlinearity and complexity of its dynamic model, this is in order to increase the control effectiveness.*

Currently, tasks involving a high precision welding of complex forms with high characteristics are very required in industry in general. This paper introduces the modeling of the end-effector movement equations to allow a tracking of welding cords with complex forms in the acceptable working zone.

Keywords: Robotics, Welding, Modeling, Trajectory Tracking

Received: 18 September 2012, Revised 8 November 2012, Accepted 12 November 2012

1. Introduction

Currently, the welding of complex forms is very requested, for example in the railway transport where we interest more and more in arc welding control. During the production, the panels are bended according to the required forms. Due to the inaccuracy of the forming operation and the inability of a simple robot to compensate the position errors, 3D laser vision systems proved to be very competitive for the detection and the tracking of joint. The Welded groups can be complex and diversified considering the slight differences, the thickness and the boundary forms of the pieces to be welded. To solve certain problems related to the tracking of assembly forms, servo-robot laser vision systems were installed on robots handled on huge immense porticos intended to weld aluminum passenger cars, goods wagons, bogies and other assemblies.

Two arc welding robots handled on a portico aimed to weld the roof and its arc in the form of saddle. It would be impossible for robots which are not endowed with vision to perform the necessary angle welding, owing to the difficulty in assembling, supporting and positioning these immense pieces with enough precision under a portico of 20 m x 6 m.

The welding of apparatuses with pressure and reservoirs is performed by devoted welding machines when they are cylindrical,

and by articulated robots in other cases.

Some big stainless steel or aluminum reservoirs used for transporting liquids through highway use joints detectors to locate preformed holes precisely, correct the robot programmed trajectory and measure the spacing in order to optimize the welding parameters.

For the welding of pieces in mechano-welding, classic machines typically look like milling machines having rotation tool and animated by relative movements in comparison with a piece firmly fixed on a table or on a support are used for the realization of simple forms welding cord.

Some machines, such as the digital milling machines, can have 5 axes to accomplish complex cord geometries ('*Gaussian forms*'). The necessary efforts for the welding operation require the machines to have a rigid structure. In general, these machines have a human/machine interface allowing the parameterization of the tool applied effort or the welding penetration depth following an axis, as well as the trajectory of the welding head.

This type of equipment allows ensuring the repetitiveness the process control of the industrial applications. In the frame of Microsoud project, Cewac, Centre of Services Study and of Applied Researches to the advantage company, acquired a new welding robot for its micro-welding platform. It will allow accomplishing even more complex 3D forms welding.

The Desmarais and Gagné Inc. au Québec [1] achieved a positioning robot for the welding of complex and irregular form with very high quality and high precision. This robot allows a better control of the temperature in order to reduce the pieces distortions.Haut du formulaire.

The car industry is the main application field of the Wolf laser robots. These robots are used for the welding of components of small or medium size. The laser welding is adapted there because the result is perfectly airtight, what protects the sensitive pieces against liquids and dusts. Besides, laser technology allows welding pieces having complex geometric forms.

There are also anthropomorphizing robots working in learning mode intended to paint complex form pieces and studied for every application area. During the direct auto-learning programming, the user manually guides the robot in a complete pulverization cycle on a sample piece using a lever.

The control computer save all trajectories and carried out commands then repeat them truthfully with the desired running speed. This method tremendously facilitates the use of the robot because the user can control the program which is memorizing and eventually correct its possible errors during the sample piece machining without problems.

After, having introduced some applications and some means used in robotized welding, the necessity to introduce some works relate to this research field.

In literature, a little works were developed to solve the problem of tracking simple and complex curves. In [2] an approach which tracks the evolution of an implicit function versus time was accomplished; the zero level corresponds to the origin or to the initial position defining the boundary of the curve.

This approach is flexible and stable, but it is too slow for real time applications. In effect, in this method the updating requires the calculation of function for all points of the curve or of the surface. In general, the tracking starts by the determination of the boundary to be followed. We pointed out that if the initial boundary is not defined, the tracking algorithm risks hard failing. As a result, the development of a quick and efficient algorithm is of big importance.

In [3] a comparison of tools machines and robots during the pieces machining was treated, an analysis of the influence of the machine or the robot mechanical behaviour on task was made; the performances of the task realization quality were modeled, simulated and assessed. In the conclusion, the taking into consideration of the triplet task/Haut du formulaire machine/commands was proposed, i.e., to define new criteria allowing qualifying the influence of the structure on the task realization quality, the

control law adaptation to the structure and to the constraints task.

In this paper we propose a method to solve the problem of tracking of curve and surfaces containing a multitude of welding cords. It allows accomplishing quick prototypes of welding techniques [4]; it is quick in the standard algorithm calculation.

The paper is organized as follows: the second point is dedicated to the problematic; in the third point we introduce the methods for models solving; the fourth point gives the generalized coordinates variation laws, whereas the fifth point is dedicated to the inverse dynamic model of manipulator robots for complex forms tracking, and we end by a conclusion and perspectives.

2. Problematic

Actually, in the majority of mechanical systems such as industrial robots and mobiles robots with embarked structures, the weight of the end-effector largely exceeds that of the supported load, thus the algorithms of these systems must be designed basing on their dynamic models; moreover, the synthesis of an autonomous arm control algorithm must be realized by taking into account the nonlinearity and the complexity of its dynamic model, this in order to increase the control efficiency.

The dynamic equation of the end-effector movement of a manipulator mechanism can be given by (1):

$$\ddot{\vec{q}}(t) = \vec{f}(\vec{q}, \dot{\vec{q}}, \vec{M}) \tag{1}$$

Where: $\vec{q}$, $\dot{\vec{q}}$ represent the generalized position and speed coordinates,

$\vec{M}$: the vector of forces and moments.

The end-effetor acceleration can be given by (2):

$$\ddot{\vec{x}}(t) = \vec{J}(\vec{q})\,\ddot{\vec{q}}(t) + \vec{P}(\vec{q}, \dot{\vec{q}}) \tag{2}$$

Where:

$\vec{x}(t)$: represents the coordinate's vector of an end-effector point,

$\ddot{\vec{q}}$: represents the generalized acceleration coordinates vector of the end-effector point,

$\vec{J}(\vec{q})$: Jacobain matrix,

$\vec{P}(\vec{q}, \dot{\vec{q}})$: the vector of the load supported by the end-effector.

From the formula (2) we obtain:

$$\ddot{\vec{q}}(t) = \vec{J}^{-1}(\vec{q})\left[\ddot{\vec{x}}(t) - \vec{P}(q, \dot{\vec{q}})\right] \tag{3}$$

3. Models Solving Method

The aim is to determine the generalized coordinates φ_p, S_p, L_p of the manipulator shown in Figure 1, by using the successive approximation method.

By drawing up the Denavit and Hartenberg table, we obtain the passage matrices A_i (i = 1, 2, 3). The general case transformation matrix is:

$$T_n = \begin{bmatrix} (t_n)_{11} & (t_n)_{12} & (t_n)_{13} & (t_n)_{14} \\ (t_n)_{21} & (t_n)_{22} & (t_n)_{23} & (t_n)_{24} \\ (t_n)_{31} & (t_n)_{32} & (t_n)_{33} & (t_n)_{34} \\ 0 & 0 & 0 & 1 \end{bmatrix} \tag{4}$$

$$A_1 = \begin{bmatrix} \cos\varphi_1 & -\sin\varphi_1 & 0 & 0 \\ \sin\varphi_1 & \cos\varphi_1 & 0 & 0 \\ 0 & 0 & 1 & 0 \\ 0 & 0 & 0 & 1 \end{bmatrix} \quad (5)$$

The product of the transformation matrices A_i (i = 1, 2, 3) will be:

$$T_3 = \begin{bmatrix} -\cos\varphi_1 & 0 & -\sin\varphi_1 & S_3\sin\varphi_1 \\ -\sin\varphi_1 & 0 & \cos\varphi_1 & S_3\cos\varphi_1 \\ 0 & 1 & 0 & L_2 \\ 0 & 0 & 0 & 1 \end{bmatrix} \quad (6)$$

$(t_n)_{\mu v}$: represents the elements of the matrix T_n.

The last column represents the end-effector position.

The coordinates of the point are given by:

$$\begin{cases} x_0 = -S_3\sin\varphi_1 \\ y_0 = S_3\cos\varphi_1 \\ Z_0 = L_2 \end{cases} \quad (7)$$

This equation system allows us to obtain the inverse kinematic solution as follow:

$$\varphi_1 = arctg\left(\frac{x_0}{y_0}\right);\ \ L_2 = Z_2;\ \ \ S_3 = \pm\sqrt{x_0^2 + y_0^2} \quad (8)$$

3.1 Inverse Kinematic Model Solving Using Successive Approximation Method

It is not often possible to solve the inverse kinematic model by analytical methods, thus we use other methods which enable us to control calculations. In the following, we present this method of transcendences equation systems solving.

The problem consists to find the value of m generalized coordinates as function of m given elements of the matrix T_n so that: $m \leq 6$.

In the case where we consider the robot have six degrees of freedom (6DOF), in this case $m = n = 6$ and we have six unknowns which are $(q_1,..., q_6)$we suppose that the elements which are in the right and above the diagonal of $T_n$matrix are known; i.e., the elements of the following matrix:

$$T_n = \begin{bmatrix} . & (t_n)_{12} & (t_n)_{13} & (t_n)_{14} \\ . & . & (t_n)_{23} & (t_n)_{24} \\ . & . & . & (t_n)_{34} \\ . & . & . & . \end{bmatrix} \quad (9)$$

For zero order approximation, the arbitrary generalized coordinates in the starting point are $(q_1^{(0)}, q_2^{(0)}, q_3^{(0)}, q_4^{(0)}, q_5^{(0)}, q_6^{(0)})$

The matrix T_n as function of the generalized coordinates in form of Taylor development for n = 6 and limiting to the linear model will be:

$$T_6 = T_6^{(k-1)} + \sum_{j=1}^{6} \frac{dT_6^{(k-1)}}{dq_j}(q_j^{(k)} - q_j^{(k-1)}) \quad (10)$$

Where

k : represents the interpolation number,

T_6^{k-1} : is an element of T_6 matrix expressed by the approximate value of the generalized coordinates.

In the case where the manipulator has $n < 6DOF$ and the number of the generalized coordinates unknown are equal to n, the linear equation system can be written under the form (11):

$$(t_n)_{\mu v} = (t_n^{(k-1)})_{\mu v} + \sum_{j=1}^{n} (t_n)_{v\mu}^{(k-1)} (q_j^{(k)} - q_j^{(k-1)}) \tag{11}$$

The application for the case of 3DOF robot, of type RTT is shown in Figure 1. The position of the end-effector is M ($x_0 = 30$, $y_0 = 100$, $z_0 = 120$).

3.2 Generalized Coordinates Determination Using Successive Approximation Method

From formula (4) we obtain:

$$(t_3)_{14} = 30.. \ (t_3)_{24} = 100.. \ (t_3)_{34} = 120 \tag{12}$$

The matrix obtained from the derivation with respect to (q_1, q_2, q_3) will be:

$$u_{31} = \begin{bmatrix} \sin q_1 & 0 & -\cos q_1 & -q_3 \cos q_1 \\ -\cos q_1 & 0 & -\sin q_1 & -q_3 \sin q_1 \\ 0 & 0 & 0 & 0 \\ 0 & 0 & 0 & 0 \end{bmatrix};$$

$$u_{32} = \begin{bmatrix} 0 & 0 & 0 & 0 \\ 0 & 0 & 0 & 0 \\ 0 & 0 & 0 & 1 \\ 0 & 0 & 0 & 0 \end{bmatrix} \quad u_{33} = \begin{bmatrix} 0 & 0 & 0 & -\sin q_1 \\ 0 & 0 & 0 & \cos q_1 \\ 0 & 0 & 0 & 0 \\ 0 & 0 & 0 & 0 \end{bmatrix}; \tag{13}$$

The last column of the matrix (3) gives

$$(t_3)_{14} = -q_3 \sin q_1; \ (t_3)_{24} = q_3 \cos q_1; \ (t_3)_{34} = q_2 \sin q_1 \tag{14}$$

The system (8) in this case accepts the form (15):

$$(t_n)_{\mu 4} = (t_3^{(k-1)})_{\mu 4} + (u_{31}^{(k-1)}) \ (q_1^{(k)} - q_1^{(k-1)}) + (u_{32}^{(k-1)})_{\mu 4} (q_2^{(k)} - q_2^{(k-1)}) + (u_{33}^{(k-1)})_{\mu 4} (q_3^{(k)} - q_3^{(k-1)}) \tag{15}$$

Taking into account of (12) and (14) and giving to μ the values 1, 2 and 3 successively we obtain the result (16)

$$\begin{aligned} 30 &= -q_3^{(k-1)} \sin q_1^{(k-1)} - q_3^{(k-1)} \cos q_1^{(k-1)} (q_1^{(k)} - q_1^{(k-1)}) + 0 (q_2^{(k)} - q_2^{(k-1)}) - \sin q_1^{(k-1)} (q_3^{(k)} - q_3^{(k-1)}) \\ 100 &= -q_3^{(k-1)} \cos q_1^{(k-1)} - q_3^{(k-1)} \sin q_1^{(k-1)} (q_1^{(k)} - q_1^{(k-1)}) + 0 (q_2^{(k)} - q_2^{(k-1)}) - \cos q_1^{(k-1)} (q_3^{(k)} - q_3^{(k-1)}) \\ 120 &= q_2^{(k-1)} + 0 \ (q_1^{(k)} - q_1^{(k-1)}) + 1 (q_2^{(k)} - q_2^{(k-1)}) + 0 (q_3^{(k)} - q_3^{(k-1)}) \end{aligned} \tag{16}$$

We have obtained for the first sizes:

$$q_1^{(0)} = 0; \ q_2^{(0)} = 0; \ q_3^{(0)} = 0.$$

From (16) arise that: $30 = 0$; $100 = q_3^{(0)}$; $100 = q_2^{(1)}$;

The obtained system does not have a solution. The presented example explains that any initial size is suitable. But it explains also that the choice of the size sets is not important. For $q_3 = 0$; the rotation of the 1st articulation with an angle q_1 does not modify the end-effector centre position in any case (such that the orientation changes). Thus, we must take the suitable positions for our manipulator robot. In this case, we take:

$$q_1^{(0)} = 0; \ q_2^{(0)} = 0; \ q_3^{(0)} = 50.$$

For $k = 0$ putting these values in (16) we obtain:

$$30 = -50q_1^{(1)};\ 100 = 50 + (q_3^{(1)} - 50);\ 120 = q_2^{(1)} \text{ and which gives us:}$$

$$q_1^{(1)} = -0.60;\ q_2^{(1)} = 120.00;\ q_3^{(1)} = 100.00.$$

For $k = 2$, the 2^{nd} approximation:

$$30 = -100 \sin(-0.6) - 100 \cos(-0.6)(q_1^{(2)} + 0.6) - \sin(-0.6)(q_3^{(2)} - 100);$$

$$100 = 100 \cos(-0.6) - 100 \sin(-0.6)(q_1^{(2)} + 0.6 + \cos(-0.6)(q_3^{(2)} - 100)$$

$$120 = 120 + (q_2^{(2)} - 100) \qquad (17)$$

which gives :

$$q_1^{(2)} = -0.283;\ q_2^{(2)} = 120.00;\ q_3^{(2)} = 99.47.$$

For $k = 3$, the 3^{rd} approximation:

$$30 = -99.47 \sin(-0.283) - 99.47 \cos(-0.283)(q_1^{(3)} + 0.283) - \sin(-0.283)(q_3^{(3)} - 99.47)$$

$$100 = 99.47 \cos(-0.283) - 99.47 \sin(-0.283)(q_1^{(3)} + 0.283 + \cos(-0.283)(q_3^{(3)} - 99.47)$$

$$120 = 120 + (q_2^{(3)} - 120) \qquad (18)$$

which gives :

$$q_1^{(3)} = -0.292;\ q_2^{(3)} = 120.00;\ q_3^{(3)} = 104.40;$$

For $k = 4$, the 4^{th} approximation: q_1 value becomes smaller than 10^{-3} and q_3 smaller, which explain the end the calculation process.

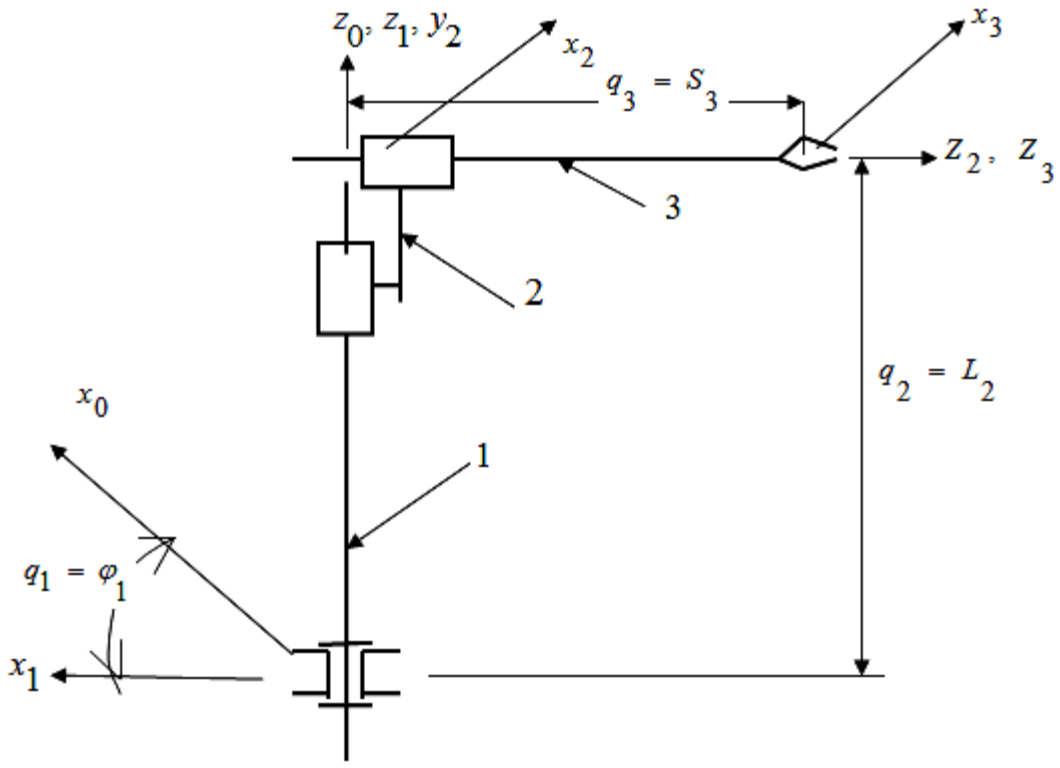

Figure 1. 3DOF manipulator robot

4. The Determination of the Generalized Coordinates Variation Law Corresponding to the end - Effector Displacement Following A Given Trajectory

4.1 Rectilinear Trajectory

Let's τ be the trajectory length traveled by the end-effector, δl is the small necessary displacement for describing the trajectory set, n_i is the corresponding intervals number, l is the traveled distance during one interval of period t_l.For better approximation, it is necessary to choose the smallest possible time interval (t_0, t_1). At the time $t_0$the generalized coordinates are known and at the end of this interval, i.e., at time $t_1$we know the end-effector position. As the generalized coordinates corresponding to time are obtained, we can use them for obtaining that which corresponds to time and so on.

The generalized coordinate corresponding to (t_1, t_2) is given by the formula (19):

$$q_j^{(0)}(t_l) = q_j(t_{l-1}) + (q_j(t_{l-1})) - (q_j(t_{l-2}))\frac{t_l - t_{l-1}}{t_l - t_{l-2}} \quad (19)$$

After having defined the calculation precision, there exists a case where the calculation volume is minimal when the interval number n_i is very high, the inverse kinematic model calculation loop is higher, in contrast, the imposed precision can be attained by the 1^{st} approximation. If n_i is small, the inverse kinematic model calculation number will be weak, in the contrary, the precision can be attained by the 2^{nd} approximation.

Let's determine the generalized coordinate's variation law of the robot shown in Figure 1; we suppose that the end-effector move following a rectilinear trajectory passing by two A and B as shown in Figure 2.

Putting $n_i = 10$ and solving the inverse kinematic model by using the preceding formulas, the results are presented on table 1. The table 1 shows that the generalized coordinates are obtained by the 1^{st}, 2^{nd} *and the* 3^{rd} approximation. The initial approximations started for $l = 2$, calculated from the formula (19). For q_2 the 1^{st} approximations give precise results yet. For q_1 and q_3 the 2^{nd} approximation gives a sufficient precision at the first and the last point; for the points existing in the middle of the trajectory where q_1 decrease, it is necessary to use the 3^{rd} approximation.

4.2 Helicoïdal Trajectory [5]

Considering the case where the trajectory to be tracked is helicoidally (Figure 3). R is the radius and b is the helices step

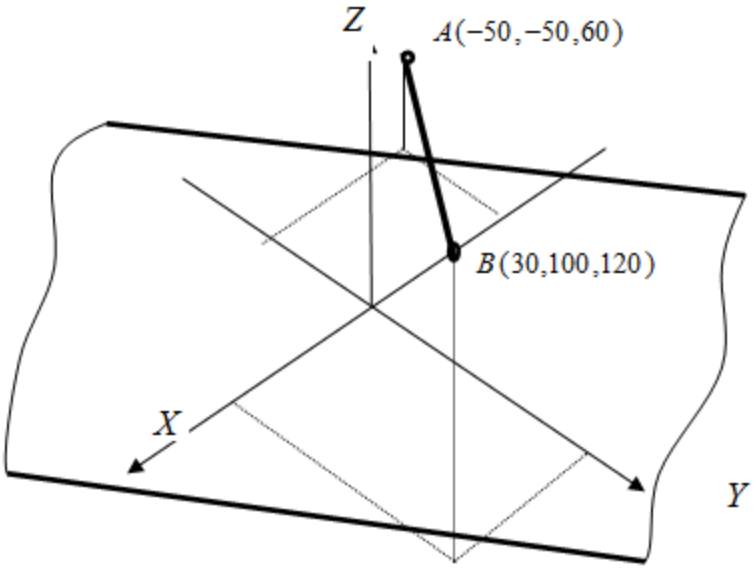

Figure 2. The end-effector displacement following AB

l	0	1	2	3	4	6	8	10
x	30	22	14	6	-2	-1	-34	-50
y	100	85	70	55	40	80	-20	-50
z	120	114	108	102	96	84	72	60
q_1	120	114	108	102	96	84	72	60
$q_1^{(0)}$	-0.292	-0.292	-0.215	-0.141	-0.020	0.711	2.458	2.429
$q_1^{(1)}$	-0.292	-0.259	-0.197	-0.108	-0.051	1.226	2.034	2.355
$q_1^{(2)}$	-0.292	-0.253	-0.197	-0.109	-0.050	1.054	2.107	2.356
$q_1^{(3)}$	-0.292	-0.253	-0.197	-0.109	-0.050	1.054	2.102	2.356
$q_3^{(0)}$	104,40	104,40	71.20	54.97	39.26	13.30	32.36	69.89
$q_3^{(1)}$	104,40	87 .74	71.38	55.30	39.95	19.53	36.98	70.53
$q_3^{(2)}$	104,40	87 .80	71.39	55.33	40.05	20.32	39.30	70.71
$q_3^{(3)}$	104,40	87 .80	71.39	55.33	40.05	20.59	39.45	70.71

Table 1. The inverse kinematic model results

v is the displacement speed to describe the trajectory. The helices parametric equations in the landmark (X_T, Y_T, Z_T) are:

$$r(\varphi)=\begin{cases} X_0 = R\cos\varphi \\ Y_0 = \dfrac{b\varphi}{2\pi} \\ Z_0 = R\sin\varphi \end{cases}$$

In the contrary, in fixed landmark it will be:

$$\vec{p}(\varphi)=\begin{cases} X_T = x = -l_1 + R\cos\varphi \\ Y_T = y = -l_2 + \dfrac{b\varphi}{2\pi} \\ Z_T = z = -l_3 + R\sin\varphi \end{cases}$$

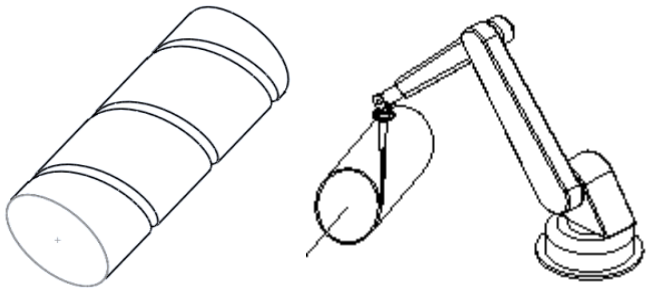

Figure 3. 2DOF helicoidally welding Robot

$$\vec{\dot{p}}(\varphi)=\begin{cases} \dot{x} = -R\dot{\varphi}\sin\varphi \\ \dot{y} = \dfrac{b\dot{\varphi}}{2\pi} \\ \dot{z} = R\dot{\varphi}\cos\varphi \end{cases}.$$

R Calculation:

$$\dot{x}^2 + \dot{y}^2 + \dot{z}^2 = \dot{\varphi}^2 R^2 + \frac{b^2\dot{\varphi}^2}{4\pi^2} = v^2$$

$$\dot{\varphi} = \frac{2\pi v}{\sqrt{4\pi^2 R^2 + b^2}}$$

By integrating this variable versus time t we obtain :

$$\dot{\varphi} = \frac{2\pi v}{\sqrt{4\pi^2 R^2 + b^2}} t + \varphi_0 .$$

Determination of the Frenet trihedral [5] (shown in Figure 4) :

$$\vec{e}_T = \frac{\vec{p}}{||\vec{p}||} = \frac{4\pi^2}{\sqrt{4\pi^2 R^2 + b^2}} \begin{bmatrix} -R \sin ct \\ \frac{b}{2\pi} \\ R\cos ct \end{bmatrix} = \frac{c}{v} \begin{bmatrix} -R \sin ct \\ \frac{b}{2\pi} \\ R\cos ct \end{bmatrix}$$

$$\ddot{s} = \frac{\dot{\vec{p}}\,\ddot{\vec{p}}}{\dot{s}} = 0 \;\; \dot{s} = \dot{v}, \; \vec{e}_N = \frac{\ddot{\vec{p}}}{||\dot{\vec{p}}||} \;\; ks^2$$

$$\frac{\ddot{\vec{p}}}{\dot{s}^2} = \begin{bmatrix} -\frac{Rc^2}{\dot{s}^2} \cos ct \\ -\frac{Rc^2}{\dot{s}^2} \sin ct \end{bmatrix} \text{ and : } k = \left\| \frac{\ddot{\vec{p}}}{\dot{s}^2} \right\| .$$

with :

$$c = \frac{2\pi v}{\sqrt{4\pi^2 R^2 + b^2}}$$

1) The angular speed and acceleration of the trihedral:
Speed: From the Frenet-Serret theorem [6] we obtain :

$$\vec{\omega} = -\dot{s}(\tau \vec{e}_T + k\vec{e}_B) \;\; \text{with : } \tau = \frac{(\vec{p}' \wedge \vec{p}'')\, \vec{p}^{\,(3)}}{k^2} \;\; \text{and :}$$

$$\vec{p}' = \frac{\dot{\vec{p}}}{\dot{s}}, \; \vec{p}' = \frac{\ddot{\vec{p}}\dot{s} - \dot{\vec{p}}\ddot{s}}{\dot{s}^3}, \dot{s} = \|\dot{\vec{p}}\| = v, k = \|\vec{p}''\|, \; \ddot{s} = \frac{\dot{\vec{p}}\,\ddot{\vec{p}}}{\dot{s}}$$

$$\vec{p}^{(3)} = \frac{(\vec{p}^{(3)}\dot{s} - s^{(3)}\dot{\vec{p}})\,\dot{s} - 3\ddot{s}(\dddot{\vec{p}}\dot{s} - \ddot{s}\ddot{\vec{p}})}{\dot{s}^5},$$

$$\vec{p}^{(3)} = \begin{bmatrix} Rc^3 \sin ct \\ 0 \\ -Rc^3 \cos ct \end{bmatrix}$$

Acceleration:

$$\dot{\vec{\omega}} = -\ddot{\vec{s}}(\tau \vec{e}_T + k\vec{e}_B) - \dot{s}(\dot{\tau}\vec{e}_T + \dot{k}\vec{e}_B),$$

$$\vec{p}^{(4)} = \begin{bmatrix} Rc^4 \cos ct \\ 0 \\ -Rc^4 \sin ct \end{bmatrix},$$

And the matrix which describes the desired position and orientation with respect to the landmark R_0 will be:

$$\left\lfloor \vec{s}_t \;\; \vec{n}_n \;\; \vec{a}_b \;\; \vec{p} \right\rfloor = \left[\vec{e}_t \;\; \vec{e}_n \;\; \vec{e}_b \;\; \vec{p} \right] E^{-1}$$

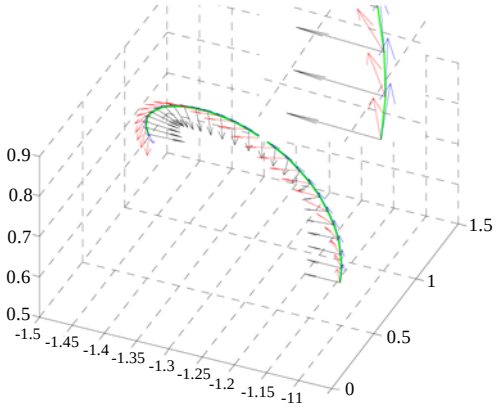

Figure 4. The trihedral vector of Frenet for the helicoidally trajectory

By using the inverse kinematic model calculation algorithm we obtain the articulated deflections. The articulated parameters allow the end-effector to follow a helecoidal trajectory.

4.3 Case of a curve given by their movement equations

In the majority of industrial robots, the end-effector weight widely exceeds the load supported by it. Thus, the necessity of taking into account of the effect of this weight in order to increase the efficiency of the robot control.

The movement of a 2*DOF* manipulator (Figure 5) is described by the following expressions:

$$a_{11}\ddot{q}_1 + a_{12}\ddot{q}_2 = M_1$$
$$a_{21}\ddot{q}_1 + a_{22}\ddot{q}_2 = M_2$$

where:

$$a_{11} = m_1.l_1 + J_1 + 4m_2l_1^2 + J_1 + l_2m_2 + 4ml_1l_2\cos q_2 + J_2$$

$$a_{12} = m_2.l_2^2 + 4m_2l_1l_2\cos q_2 + J_2$$

$$M_1 = M_1' + 2m_2l_1l_2\sin q_2\,\dot{q}_1^2 + 2m_2l_1l_2\sin q_1\,q_2$$

$$a_{21} = m_2.l_2^2 + 2m_2l_1l_2\cos q_2 + J_2$$

$$a_{22} = -(m_2.\,l_2^2 + J_2)$$

$$M_2 = M_1' + 4m_2l_1l_2\sin q_2\,\dot{q}_1\dot{q}_2 + 2m_2l_1l_2\sin q_2\,\dot{q}_1^2$$

l_1, l_2 : the length of the link,

m_1, m_2 : the weight of the link,

J_1, J_2 : the inertial moments,

M_1, M_2 : motors moments,

M_1', M_2': the moments exerted on the articulations 1 and 2,

So, the functions $f_1(\vec{q}, \vec{\dot{q}}, \vec{M})$ and $f_2(\vec{q}, \vec{\dot{q}}, \vec{M})$ which enter into the equation are presented under the form:

$$f_1(\vec{q}, \vec{\dot{q}}, \vec{M}) = (M_1a_{22} - M_2\,.\,a_{12}) / \Delta f$$
$$f_2(\vec{q}, \vec{\dot{q}}, \vec{M}) = (M_2a_{11} - M_1\,.\,a_{21}) / \Delta f \qquad (16)$$

where: $\Delta f = a_{11}.\, a_{22} - a_{12}.\, a_{21}$

From the kinematic equations of the manipulator we find:

$$\ddot{x}_1 = -l_1.\, cos\, q_1 \dot{q}_1^2 - x_2\,.\,\ddot{q}_1 - l_2.\, \cos(q_1 - q_2)\,.\,(\dot{q}_1 + \dot{q}_2)^2 - l_2.\, \sin(q_1 + q_2)\,\ddot{q}_2$$

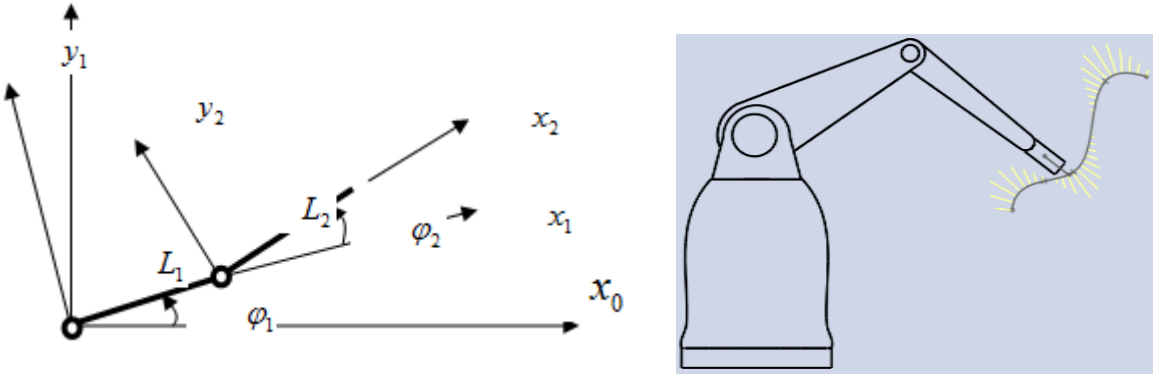

Figure 5. Schéma d'un manipulateur plan à 2DDL

$$\ddot{x}_2 = x_1.\, \dot{q}_1 - l_2.\, \cos(q_1 + q_2)\,.\,\dot{q}_2 - l_1\,.\,\sin\dot{q}_1^2 - l_2.\, \sin(q_1 + q_2)\,(\dot{q}_1 + \dot{q}_2)^2 \qquad (17)$$

Thence we determine the Jacobian matrix and the kinematic functions:

$$J_{(\vec{p})} = \begin{bmatrix} -x_2 - 2.l_2.\, \sin(q_1 + q_2) \\ x_1 - 2.l_2.\, \cos(q_1 + q_2) \end{bmatrix}$$

$$P_{1(\vec{q},\vec{\dot{q}})} = -\,l_1\,.\,\cos q_1.\, \dot{q}_1^2 - l_2\,.\,\cos(q_1 + q_2)\,.\,(\dot{q}_1 + \dot{q}_2)^2$$

$$P_{2(\vec{q},\vec{\dot{q}})} = -\,l_1\,.\,\sin q_1.\, \dot{q}_1^2 - l_2\,.\,\sin(q_1 + q_2)\,(\dot{q}_1 + \dot{q}_2)^2 \qquad (18)$$

According to equation (7) and taking into account (16) we writ the prescribed value expression of the function $f^*(\vec{q}, \dot{\vec{q}}, \vec{M}^*)$;

$$\frac{1}{\Delta f}\begin{bmatrix} M_1^*.\, a_{22} - M_2^*.\, a_{12} \\ M_2^*.\, a_{11} - M_1^*.\, a_{21} \end{bmatrix} = \frac{1}{\Delta}\begin{bmatrix} 2.l_2.\, \cos(q_1 + q_2)\, x_1 \\ 2.l_2.\, \sin(q_1 + q_2) - x_2 \end{bmatrix} X$$

$$X \begin{bmatrix} (k_{11}.\, \dot{x}_1 - k_{12}\,(x_1 - x_1) - p_{1(q,\dot{\vec{q}})}) \\ (k_{21}\dot{x}_2 - k_{22}\,(x_2 - x_2) - p_{2(q,\dot{\vec{q}})}) \end{bmatrix} \qquad (19)$$

By solving (19) with respect to M_1^*, M_2^* we obtain:

$$M_1^* = a_{11}\,;\, D_1 + a_{12}\,;\, D_2$$

$$M_2^* = a_{11}\,;\, D_1 + a_{12}\,;\, D_2$$

where:

$$D_1 = \{2l_2.\, \cos(q_1 + q_2)\,.[k_{11}\dot{x}_1 - k_{12}.(x_1^* - x_1) - P_1(q, \dot{q})]$$

$$+ x_1.[k_{21}.\, x_2 - k_{22}\,(x_2^* - x_2) - P_2(q, \dot{q})]\}/\Delta$$

$$D_2 = \{2l_2.\, \sin(q_1 + q_2)\,.[k_{11}\dot{x}_1 - k_{12}.(x_1^* - x_1) - p_1(q, \dot{q})]$$

$$+ x_1.[k_{21}.\, x_2 - k_{22}\,(x_2^* - x_2) - P_2(q, \dot{q})]\}/\Delta$$

We find also the required motor moments:

$$M_1'^{*} = a_{11}.D_1 + a_{12}.D_2 - 2m_2.l_1.l_2 \sin q_2.\dot{q}_2^2 - 4.m_2.l_1.l_2.\sin q_2 \dot{q}_1\dot{q}_2;$$
$$M_2'^{*} = a_{21}.D_1 + a_{22}.D_2 - 4m_2.l_1.l_2 \sin q_2.\dot{q}_1.\dot{q}_2^2 - 2.m_2.l_1.l_2.\sin q_2 \dot{q}_1^2; \quad (20)$$

For the motor functions we can write:

$$u = \frac{R_{ia}}{kk_M} M'^{*} + \frac{1}{k}[(k_\omega + k_v).\dot{q} + q]; \quad (21)$$

4.4 The tracking of any curve

Consider the case of the end-effector tracking a curve which is given by its multiple integral:

$$\varphi_1(x1, x2, xn) = 0$$

The problem is the determination of differential equations of the manipulator from the multiple integral so that the expression (21) is the integral of these equations.

Given the motion trajectory in the form:

$$\varphi_1(x_1, x_2, x_3) \text{ and } \varphi_2(x_1, x_2, x_3) \quad (22)$$

The boundary conditions are:

$$x_{(\vec{0})} = \vec{x}; \ \dot{\vec{x}}_{(0)} = 0; \ \vec{x}_{(\alpha)} = \vec{x}^{*}; \ \dot{\vec{x}}_{(\alpha)} = 0;$$

The motion equations along each coordinate are given as:

$$\vec{x}_1^{k} - \vec{x}_1(t) = C_{11}e^{\alpha_{11}t} + C_{11}e^{\alpha_{12}t};$$
$$\vec{x}_2 - \vec{x}_2(t) = C_{21}e^{\alpha_{21}t} + C_{22}e^{\alpha_{22}t}; \quad (23)$$
$$\vec{x}_3^{*} - \vec{x}_3(t) = C_{31}e^{\alpha_{31}t} + C_{32}e^{\alpha_{32}t};$$

Where: x_i^* (i = 2, 3) : represent the solution of the system (22) for a fixed value of x_1 ;

$x_i(t)$ (i = 2, 3) : represent the current coordinates of the end-effector position.

The 1st equation ensures the exponential law of the end-effector displacement from the start point to the target of x_1 coordinates.

The 2nd and 3rd equations characterize the difference between the trajectories passing through x_2 and x_3.the case (23) also guarantees the asymptotic stability of the clamp motion along a given path. By the differential of the formula (23), we find the corresponding acceleration vector.

$$\ddot{x}_1 = \alpha_{11}\alpha_{12}\lfloor x_1^k - x_1(t)\rfloor + (\alpha_{11} + x_{12})\dot{x}_1(t)$$
$$\ddot{x}_2 = \alpha_{21}\alpha_{22}\lfloor x_2^k - x_2(t)\rfloor + (\alpha_{21} + x_{22})\lfloor \dot{x}_2^{*} - \dot{x}_2\rfloor + \ddot{\vec{x}}_2^{*} \quad (24)$$
$$\ddot{x}_3 = \alpha_{31}\alpha_{32}\lfloor x_3 - x_3(t)\rfloor + (\alpha_{31} + x_{32})\lfloor \dot{x}_3^{*} - \dot{x}_3\rfloor + \ddot{\vec{x}}_3^{*}$$

$\dot{x}_i^*$ and $\ddot{x}_i^*$ values represent the 1st and the 2nd derivatives of the formula (22). Making the differential of (22) we obtain:

$$\sum_{k=1}^{3} \frac{\partial \varphi_i}{\partial x_k} \dot{x}_k^{*} = 0$$
$$\sum_{k=1}^{3} \frac{\partial \varphi_i}{\partial x_k} \ddot{x}_j^{*} = 0 + \sum_{k=1}^{3}\sum_{j=1}^{3} \frac{\partial^2 \varphi_i}{\partial x_j \partial x_k} \partial x_k \dot{x}_b \dot{x}_k = 0 \ i = 1, 2; \quad (25)$$

After we obtain : $\dot{x}_1^*$, $\dot{x}_2^*$ and $\ddot{x}_1^*$, $\ddot{x}_2^*$. as solution of the linear equations system (24); by changing in (23), $\dot{x}_2^*$, $\dot{x}_3^*$ and $\dot{x}_3^*$ from

solutions (24) we obtain the programmed acceleration of the clamp $\ddot{x}_k$, with (k = 1, 2, 3) according to the coordinates of their 1^{st} derivatives and $\ddot{x}_k^*$, is a quantity which can be loaded, using the 1^{st} equation of the system (23).

In this way the unknown acceleration of the clip, obtained by the program (22), is a function of speed and coordinates. By solving the equations (23), and (24) we find the generalized forces programmed as:

$$\vec{f}^{*}(\vec{q}, \vec{q}, \vec{M}) = J^{-1}(q)[\vec{x}(\vec{x}, \vec{x}) - P(\vec{q}, \vec{q})] \tag{26}$$

Note that the obtained function is nonlinear which allows building the control system based on the inverse relations.

$$\vec{u}^{*} = \frac{R_I}{kk_M}[J^{-1}(q)(-k_1\dot{x}_1^{*} - k_2)(\vec{x}^{*} - \vec{x}) - \vec{P}(q, \vec{q}^{*}))] + kW + kV)\,\dot{\vec{q}} + \vec{q} \tag{27}$$

Where : R_i, k_M, k_W, k_V, represent the motor parameters.

$\vec{u}^{*}$: the voltage.

The diagram of the control algorithm, realizing the motion of the manipulator along a given path is given in Figure 6.

4.5 Inverse dynamic model of manipulators for tracking of complex forms

The control algorithm construction of a manipulator for tracking a surface knowing the normal force at the contact point and the speed of movement of the end-effector (instrument) (Figure 7) is given by.

$$m_2\ddot{x} = Q_2 + N.\,\vec{n}.\,\vec{i} \tag{28}$$

$$(m_1 + m_2).\ddot{y} = -P_2 - P_2 \times Q_1 + N.\,\vec{n}.\,\vec{j} \tag{29}$$

m_1, m_2: the weight of the manipulator links;

x, y : the coordinates of the centers of mass relative to the fixed coordinate systems xoy.

P_1, P_2: the weights of the links 1 and 2,

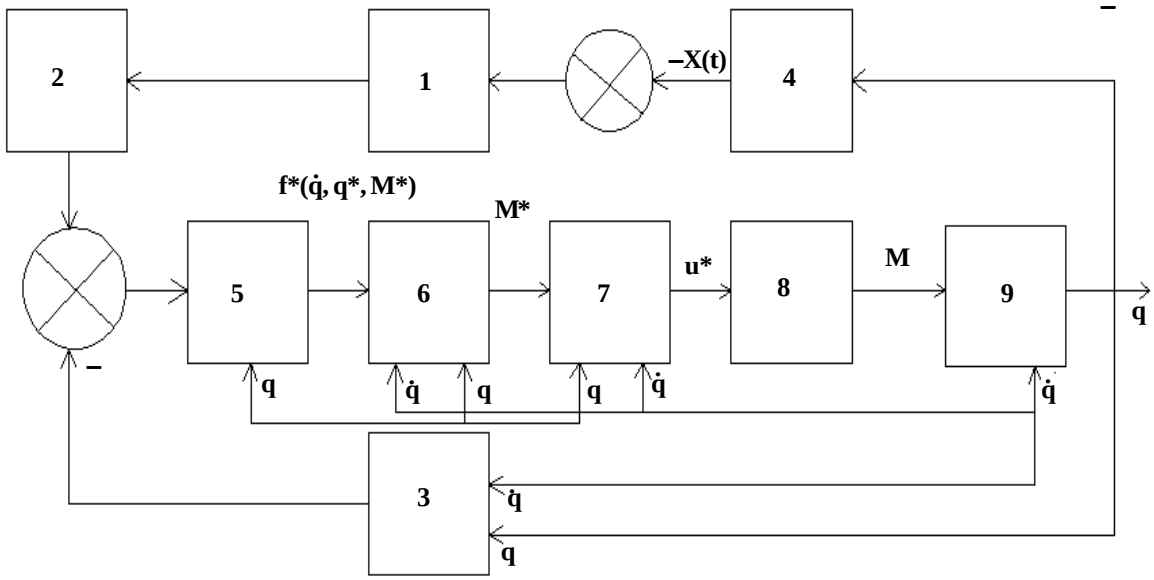

Figure 6. The structural diagram of the robot controlling algorithm for tracking a given curve

Q_1, Q_2 : active forces of the actuators,

N : the modulus of the normal force at the contact point of the end-effector with the surface,

$\vec{n}$: the vector normal to the surface, $n = \dfrac{grad\ f}{|\ grad\ f\ |}$

$f_{(x,y)} = 0$: Equation of the curve to be followed by the robot,

$\vec{i}, \vec{j}$: unit vectors,

$$grad\ f = \frac{\partial f}{\partial x}.\vec{i} + \frac{\partial f}{\partial y}.\vec{j},$$

$$\left| grad\ f = \sqrt{\left(\frac{\partial f}{\partial x}\right)^2 + \left(\frac{\partial f}{\partial y}\right)^2} \right| \tag{30}$$

$$\begin{cases} m_2\ddot{x} = Q_2 + \dfrac{N.\dfrac{\partial f}{\partial x}}{G} & (31) \\ (m_1 + m_2).\ddot{y} = -P_2 - P_2 \times Q_1 + \dfrac{N.\dfrac{\partial f}{\partial x}}{G} & (32) \end{cases}$$

with $G = |grad\ f|$

The motor differential equation:

$$\dot{u}_v = \dot{Q}_v.k_1 + Q_v.k_2 \tag{33}$$

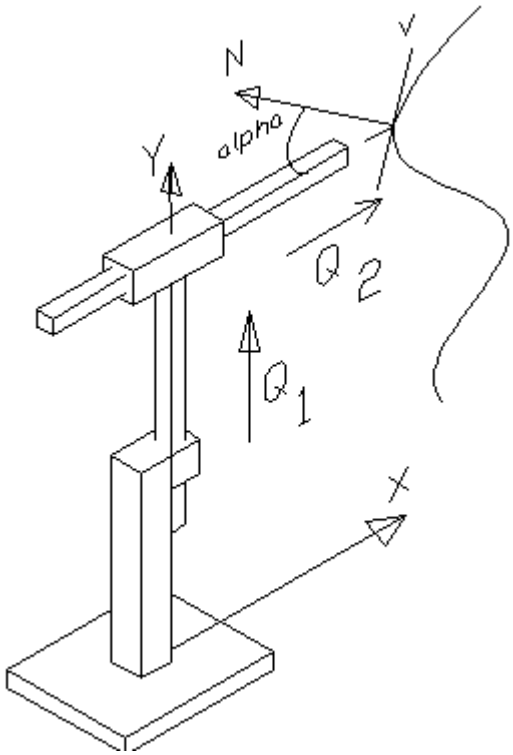

Figure 7. Robot diagram for tracking a complex 2D curve

u_v : control voltage in *v. m*

k_1, k_2 : constant coefficient characterizing the motors, from (31) we find the expression of Q_2 ,

$$Q_2 = -N.\frac{\partial f}{\partial x}\Big/ G + m_2\ddot{x} \tag{34}$$

Taking the differential (34),

$$\dot{Q}_2 = -N\frac{\frac{\partial f}{\partial x}}{G} - \frac{N.\left(\frac{\partial^2 f}{\partial x^2}.\dot{x} + \frac{\partial^2 f}{\partial y^2}.\dot{y}\right).\left[1-\left(\frac{\partial f}{\partial x}\right)^2/G^2\right]}{G} - \frac{N.\frac{\partial f}{\partial x}.\frac{\partial f}{\partial y}.\left(\frac{\partial^2 f}{\partial x \partial y}.\dot{x} + \frac{\partial^2 f}{\partial y^2}.\dot{y}\right) + m_2.\ddot{x}}{G^3} \tag{35}$$

By solving (33) and (35) we obtain the expression:

$$\dot{u} = -\frac{k_1.\dot{N}.\frac{\partial f}{\partial x}}{G} - \frac{k_1.N.\left(\frac{\partial^2 f}{\partial x^2}.\dot{x} + \frac{\partial^2 f}{\partial y^2}.\dot{y}\right).\left[1-\left(\frac{\partial f}{\partial x}\right)^2/G^2\right]}{G} - \frac{k_1.N.\left(\frac{\partial f}{\partial x}.\frac{\partial f}{\partial y}.\left(\frac{\partial^2 f}{\partial x \partial y}.\dot{x} + \frac{\partial^2 f}{\partial y^2}.\dot{y}\right)\right)}{G^3} + k_1.m_2.\ddot{x} - \frac{k_2.N.\frac{\partial f}{\partial x}}{G} + k_2 m_2.\ddot{x} \tag{36}$$

$$\dot{N} = \lambda.(N - N_{pr}) \qquad \lambda < 0 \tag{37}$$

N_{pr} : the programmed normal force module,

$$\dot{u} = -\frac{k_1.\lambda}{G}.(N - N_{pr}).\frac{\partial f}{\partial x} - \frac{k_1.N}{G}.\left(\frac{\partial^2 f}{\partial x^2}.\dot{x} + \frac{\partial^2 f}{\partial y^2}.\dot{y}\right).\left[1-\left(\frac{\partial f}{\partial x}\right)^2/G^2\right] + \frac{k_1.N.\left(\frac{\partial f}{\partial x}.\frac{\partial f}{\partial y}.\left(\frac{\partial^2 f}{\partial x \partial y}.\dot{x} + \frac{\partial^2 f}{\partial y^2}.\dot{y}\right)\right)}{G^3} + k_1 m_2.\ddot{x} - \frac{k_2.N.\frac{\partial f}{\partial x}}{G} + k_2 m_2.\ddot{x} \tag{38}$$

We obtain :

$$\dot{u} = -k_1.\lambda.(N - N_{pr}).\frac{\partial f}{\partial x}/G + k_2.Q_2 + k_1.\dot{Q}_2 + k_1.N.\frac{\partial f}{\partial x}/G \tag{39}$$

To ensure the tracking of the trajectory along a curve given by its equation and respecting the normal force acting on the end-effector we have to choose an actuator delivering a load of $\vec{Q}_2$.

$$\dot{v} = \gamma.(v - v_{pr}) \qquad \gamma < 0 \tag{40}$$

This formula guarantee the stability of the value of the end-effector motion speed relative to the surface.

$$v = \sqrt{\dot{x}^2 + y^2} \tag{41}$$

v : the speed module,

$\dot{x}, \dot{y}$: the projection of the speed v along the axes of the coordinate system,

Deriving (14) with respect to time yields:

$$\gamma.(v - v_{pr}) = \dot{x}.\dot{y}.\ddot{y}/v \tag{42}$$

Drawing y from (29) we obtain:

$$\gamma = \gamma.(v - v_{pr}) = \dot{x}.\ddot{x}/v + \dot{y}.\left(-P_1 - P_2 + Q_1 + N\frac{\partial f}{\partial x}/G\right)/(m_1 + m_2).v \tag{43}$$

Drawing $\dot{Q}_1$ from (43) we obtain :

$$\dot{Q}_2 = (m_1 + m_2)\frac{\dot{v}}{y}\left[\gamma.(v - v_{pr}) - \frac{\dot{x}.\ddot{x}}{v}\right] + (m_1 + m_2).$$

$$.\frac{v}{y}\left[\gamma.\dot{v} - \frac{\ddot{x}^2 + \dot{x}.\ddot{x}}{v}\right] - \left\{\frac{\dot{N}}{G}.\frac{\partial f}{\partial x} + \frac{N}{G}\left(\frac{\partial^2 f}{\partial x^2}.\dot{y} + \frac{\partial^2 f}{\partial y^2}.\dot{x}\right).\right.$$

$$\left.\left(1 - \left(\frac{\partial f}{\partial x}\right)^2 / G^2\right) - \frac{N}{G^3}\left(\frac{\partial f}{\partial x}.\frac{\partial f}{\partial y}\right)\left(\frac{\partial^2 f}{\partial x \partial y}.\dot{y} + \frac{\partial^2 f}{\partial y^2}.\dot{x}\right)\right\}$$

Using the formula (33) we obtain:

$$\dot{u}_2 = (m_1 + m_2)\frac{\dot{v}}{\dot{y}}\left[\gamma.(v - v_{pr}) - \frac{\dot{x}.\ddot{x}}{v}\right] + (m_1 + m_2)\frac{v}{y}\left[\gamma.\dot{v} - \frac{\ddot{x}^2 + \dot{x}.\ddot{x}}{v}\right] -$$

$$\left\{\frac{\dot{N}}{G}.\frac{\partial f}{\partial x} + \frac{N}{G}\left(\frac{\partial^2 f}{\partial x^2}.\dot{y} + \frac{\partial^2 f}{\partial x \partial y}.\dot{x}\right).\left(1 - \left(\frac{\partial f}{\partial x}\right)^2 / G^2\right) - \frac{N}{G^3}\left(\frac{\partial f}{\partial x}.\frac{\partial f}{\partial y}\right)\left(\frac{\partial^2 f}{\partial x \partial y}.\dot{y} + \frac{\partial^2 f}{\partial y^2}.\dot{x}\right)\right\}k_1 +$$

$$+ \frac{v}{y}.(m_1 + m_2)\left(\gamma.(v - v_{pr}) - \frac{\dot{x}.\ddot{x}}{v}\right) - \frac{N}{G}.\frac{\partial f}{\partial x} + P_1 + P_2\Big]k_2 \qquad (44)$$

5. Conclusion

During the execution of a tracking task, the end-effector is actually in contact with the curve or the surface. For this purpose, the kinematic structure of the robot passes from an open structure chain to an enclosed structure. Contact with the environment imposes additional kinematic and dynamic constraints that must be considered.

The approach used in the algorithm has significantly reduced the number of iterations needed to reach our result. The combination of an alternative approach has improved the robustness of the tracking algorithm.

We obtained the control formulas for tracking a curve given by its equations and can be used to tracking an area by decomposing it to parallel curves.

For future work, we state the need to continue this work to reflect the environment in which the robot will move, simulating various applications in design software. The comparison of theoretical results with practical results is highly desirable.

References

[1] Maisonneuve Granby, Québec J2G 3H5 Canada.

[2] Osher, S., Sethian, J. (1998). Fronts propagating with Curvature dependant speed: algorithms based on Hamilton-Jacobi formulation, *Journ. Computing phys*. 79, 12-49.

[3] Hélène Chanal et Flavien Paccot, Comparaison des machines outils et des robots pour l'usinage de pièces. versune convergence scientifique et technologique, LaMI, EA 3867 - FR TIMS / CNRS 2856

[4] Prototypage rapide par soudage robotisé, Antonio Fernando Ribeiro, Université de Minho, (2010), Portugal.

[5] Morin, P., et Samson, C. (2004). Commande, INRIA, Route des Lucioles 06902, Sophia-Antipolis Cedex.

[6] Walter Greiner. (2004). Classical Mecanics, point particles and relativity, Springer.